Food Chemistry 354 (2021) 129454

Contents lists available at ScienceDirect

Food Chemistry

journal homepage: www.elsevier.com/locate/foodchem

Identification of blood-red color formation in edible bird's nests provides a new strategy for safety control

Chun-Song Cheng [a,d,1], Chi-Chou Lao [a,1], Qi-Qing Cheng [a,1], Zi-Ling Zhang [a], Jing-Guang Lu [a], Jian-Xin Liu [b], Hua Zhou [a,c,*]

[a] Faculty of Chinese Medicine and State Key Laboratory of Quality Research in Chinese Medicine, Macau University of Science and Technology, Taipa, Macao, PR China
[b] School of Pharmaceutical Sciences, Hunan University of Medicine, Huaihua City, Hunan Province, PR China
[c] Joint Laboratory for Translational Cancer Research of Chinese Medicine of the Ministry of Education of the People's Republic of China, Macau University of Science and Technology, Taipa, Macao, PR China
[d] Lushan Botanical Garden, Chinese Academy of Sciences, Jiujiang City, Jiangxi Province, PR China

ARTICLE INFO

Keywords:
Blood-red edible bird's nest
UHPLC-TOF/MS
NMR
Phenol-keto tautomerism
Color change

ABSTRACT

In order to reveal the color formation mechanism of blood-red edible bird's nests (EBNs) and develop a quick and specific strategy to distinguish the artificial fake one, multiple methods of UPLC-TOF/MS, UV, NMR, FT-IR and 2D IR were used to detect the chemical markers of the reddening reaction, the results showed that the reddening substances were $C_9H_{10}N_2O_5$ and $C_9H_9NO_6$, which were verified as products of a phenol-keto tautomerism evolved from L-tyrosine. Moreover, natural and artificial red EBNs with varying degrees of chemical fumigation also can be successfully distinguished using the chemical markers, and the protein variation in SDS-PAGE gel could also support the distinction. This work established a systematic method of chemical identification for both natural and artificial blood-red EBNs, and provided a new identification strategy for food safety control that can promote the development of a healthier market of EBNs.

1. Introduction

Edible bird's nests (EBNs) are secreted by several species of *Aerodramus* genus (*Collocallia*) (Goh et al., 2000; Guo et al., 2014), such as *A. fuciphagus* and *A. maximus*, which are found mostly in Southeast Asia countries, including Thailand, Vietnam, Indonesia, Malaysia and Philippines (Lin et al., 2009; Marcone, 2005) as well as China. Because of its beneficial effects to respiratory health, energy boosting, skin regeneration and general longevity, the EBN is usually prepared as a nutrient soup, prized as a healthful delicacy, and used as a traditional Chinese medicine. It has a medicinal history of more than 300 years, and was first recorded in ancient literature "Ben Cao Bei Yao" and "Ben Cao Feng Yuan" in CE 1700 (Qing dynasty in China) (Chan, 2018; Xian et al., 2010).

The mucin glycoprotein in EBNs has a polypeptide backbone and plenty of polysaccharide chains attached to it (Shim, Chandra, Pedireddy, &Lee, 2016). It composes of lipid (0.14–1.28%), ash (2.1%), carbohydrate (25.62–27.26%) and protein (62–63%). The most abundant component of EBN is crude protein, which is made up of 17 amino acids, such as serine, valine, isoleucine, aspartic acid and asparagine, tyrosine, phenylalanine, glutamic acid, glutamine, and so on, but with the absence of tryptophan, cysteine, and proline (Marcone, 2005).

The authentication and quality control of common EBN have attracted the attention of scientists very early, and have already been established (Yang, Cheung, Li, &Cheung, 2014). But there are many different colors of EBNs presenting on the superior health food markets in China, Japan, and the other countries of Southeast Asia (Paydar et al., 2013), such as white, yellow and blood-red, as shown in Fig. 1A. In some rumors, it is generally considered that the blood-red EBNs are the nests mixed with the bird's blood, with higher nutritional or medicinal value for health, and worth more expensive price than white EBNs (Paydar et al., 2013). Amino acid analysis revealed that both white and blood-red EBNs had very similar amino acid levels, which were 63% and 62% respectively (Marcone, 2005). There is no clear evidence that the medicinal value of blood-red EBN is higher than that of white EBN. Moreover, it is proved that there is no hemoglobin in blood-red EBN, so

* Corresponding author at: Faculty of Chinese Medicine and State Key Laboratory of Quality Research in Chinese Medicine, Macau University of Science and Technology, Taipa, Macao, PR China.
E-mail addresses: chengcs@lsbg.cn (C.-S. Cheng), hzhou@must.edu.mo (H. Zhou).
[1] These authors contribute equally to this work.

https://doi.org/10.1016/j.foodchem.2021.129454
Received 7 September 2020; Received in revised form 20 February 2021; Accepted 21 February 2021
Available online 3 March 2021

the red color is not caused by blood. Studies have reported that the EBNs getting red is due to the vapors from bird soil in hot and humid conditions or a chemical reaction from the sodium nitrite ($NaNO_2$) dissolved in 2% hydrochloric acid (HCl) (But et al., 2013; Paydar et al., 2013), but the mechanism is not illuminated clearly. Recently, two studies gave different explanations about the mechanism of color change from white to red in EBNs. Wong *et al.* showed the red EBN could be caused by oxidation of Fe ions in AMCase-like proteins (Wong, Chan, Dong, & Tsim, 2018). Shim *et al.* suggested red color is the result of xanthoproteic reaction, and used a sensitive biological method, ELISA, to detect the nitration of the glycoprotein tyrosine residues to the 3-nitrotyrosyl residues, meanwhile, the color changed from yellow at low pH to deep red at high pH (Shim & Lee, 2018).

However, there is no effective way and corresponding chemical markers to identify and distinguish the natural and artificial blood-red EBNs. The process of EBN turning red is very slow and complicated, how the entire reaction proceeds, including reaction type, reaction location, reaction product, *etc*., needs further studies. Moreover, the red substance is neither water-soluble nor lipid/solvent extractable, how to obtain sufficient indicative compounds for effective chemical detection, is also an urgent problem to be solved. So, we attempt to obtain enough substrate and reveal the reddening mechanism thoroughly, thereby provide a systematic identification strategy for accurately distinguishing the artificial or natural blood-red EBNs. Our mechanism hypothesis is proposed as follows: the natural reddening reaction may occur at the peptide chain, and the depth of color can be related to the amount of chromophore and the protein conformation. As shown in Fig. 1B, the chemical reaction shows the natural or artificial color change process occurs at the peptide chain is named as Protein-Chromophore-Reaction on EBN (PCRE). Target chromophore and auxochrome are most likely derived from amino acids with aromatic groups, like tyrosine, phenylalanine and tryptophan. A substantial amount of tyrosine and phenylalanine is contained in the protein peptide chain of EBNs, and the reaction is run under room temperature, but the nitration of phenylalanine by xanthoproteic reaction needs heat, only tyrosine can react at room temperature because of ring activation by phenolic –OH, so this

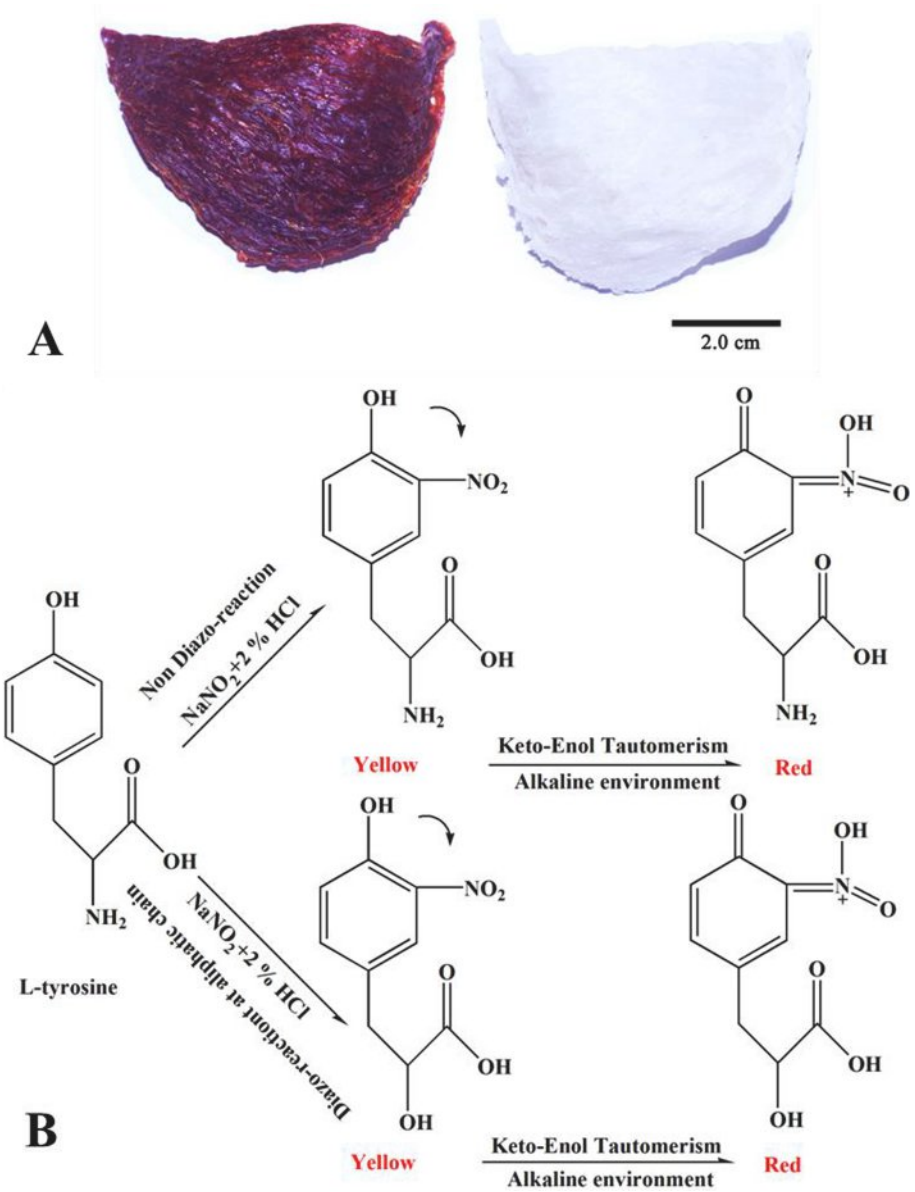

Fig. 1. Appearance of EBNs (A) and hypothesis of color formation mechanism of blood-red EBNs by taking L-tyrosine as an example (B). Theoretical chromophore and auxochrome are shown in this mechanism hypothesis, and they come from the reactions of $NaNO_2$ dissolved in 2% HCl and $NH_3{\cdot}H_2O$. (For interpretation of the references to color in this figure legend, the reader is referred to the web version of this article.)

reddening reaction is most likely to happen at tyrosine. A specific tyrosine hydrolysis reaction strategy is needed to get enough compounds for detection. In the hypothesis of color formation mechanism we proposed (Fig. 1B), two synthetic products can be obtained by fumigation using $NaNO_2$ and 2% HCl. So, a part of L-tyrosine undergoes a diazo-reaction on the aliphatic chain, and then a substitution reaction happens under the environment of HCl and H_2O (Ceriotti & Spandrio, 1957). Therefore, under the fumigation of ammonia ($NH_3{\cdot}H_2O$), the colors will be deepened by the reaction of the phenol-keto tautomerism, a kind of keto-enol tautomerism.

In this study, we used high-purity L-tyrosine compound (>99%) and L-tyrosine hydrolyzed and isolated from EBNs as substrates to explore the red color formation mechanism of blood-red EBNs, then identified the reaction process and products by multiple chemical methods, subsequently verified the reddening reaction on white EBNs. Furthermore, three kinds of scientific methods were used to identify them, including: 1) Detecting reddening ingredients by ultra-high performance liquid chromatography with tandem quadruple time of flight mass spectrometer technology (UHPLC-TOF/MS), nuclear magnetic resonance H spectroscopy (^{1}H NMR), UV spectrophotometer and infrared spectroscopy (IR); 2) Detecting protein cleavage using SDS-PAGE protein electrophoresis; and 3) Detecting synergies of different chemical groups using 2D IR. These methods verified the reliability and accuracy of each other, thereby proving the hypothesis and further confirming the chemical markers. As LC-TOF/MS has been proved to be a sensitive and stable detection method for trace compounds in food (Ferrer & Thurman, 2007), in actual application, UHPLC-TOF/MS would be the most intuitive and preferred one among our methods. Our aim was to discover the mechanism of natural and artificially fumigated EBNs turning red, identify the chemical markers of reddening reaction and establish a systematic chemical method for quality control of blood red EBNs, no matter natural or artificial one. Therefore, the reddening mechanism of EBNs should be clearly understood, and strong evidence could be provided for customers and market to identify red EBNs and determine the value effectively.

2. Materials and methods

2.1. Edible bird's nest (EBN) samples and chemicals

Standard EBN samples were purchased from Tongrentang pharmacy (Bozhou, Anhui, China), testing EBN samples were bought from market in Bozhou, Anhui, China in 2014, and then they were labeled and stored at room temperature upon arrival. Carboxypeptidase A (CPA) was purchased from Sigma-Aldrich (St. Louis, MO, USA). L-tyrosine was purchased from the institute of Xinxing Chemical Engineering (Shanghai, China). $NaNO_2$ and HCl were purchased from Fuchen Chemical Reagents Factory (Tianjin, China).

2.2. Reddening reaction of L-tyrosine and white EBN

According to Wong's method, white EBNs exposed to vapor from $NaNO_2$ and 2% HCl could turn red (But et al., 2013; Paydar et al., 2013). So one gram of $NaNO_2$ and a tube of one milliliter of saturated L-tyrosine aqueous solution were fixed on the bottom of a transparent jar, and 2% HCl was added to a depth of 1 cm in the jar. A filter paper, filled with $NH_3{\cdot}H_2O$, was hanged at the top of the jar and maintained not to stain the solution. The jar was sealed and placed into the fume hood to keep the reaction for 48 h. Similar to the L-tyrosine reaction steps, white EBN was reacted in another jar according to the above steps.

2.3. UV spectrophotometer analysis

After reddening reaction, L-tyrosine solution was reacted from transparent solution to yellow solution in the early stage, and red solution later. Using water as the blank, the yellow and red L-tyrosine solutions were diluted 100 times respectively. Then they were put into a quartz cuvette and scanned from 800.0 nm to 200.0 nm by Cary60-UV spectrophotometer (Agilent Technologies, Santa Clara, USA) to record the absorption spectra.

2.4. Paper chromatography isolation

Filter paper was cut into rectangular shape (20 cm × 30 cm), and sample solutions were spotted along a straight line 2 cm from the bottom edge. Thirty milliliters developing solvent consisting of *n*-butanol:acetic acid:water (4:1:5, upper phase) was poured into a 2000 mL glass storage jar. After sealing and saturation, the filter paper was put into the jar. When the solvents ran out of the top of the filter, the separation was completed, and the color was also separated.

2.5. Enzymatic hydrolysis using CPA

L-tyrosine can be obtained from EBNs by a specific hydrolysis reaction using CPA (Fig. S1, see supplementary materials) (Christianson & Lipscomb, 1989; Quiocho & Lipscomb, 1971). The powders of EBNs were moved into 10 mL centrifuge tubes after grinding, and then sterile water (3 mL) was added till the pH was 7.5. Two milligrams of CPA were added in each tube to perform the hydrolysis reaction overnight at 4 °C. Hydrolysis products (20 μL) were diluted for 50 times and stored at 4 °C.

2.6. UHPLC-TOF/MS analysis

The UHPLC-TOF/MS analysis was performed at an Agilent 1290 Infinity UHPLC system (Agilent Technologies, Santa Clara, USA) coupled with an Agilent 6230 Accurate Mass Time-of-Flight Mass Spectrometer system (Agilent Technologies, Santa Clara, USA). The raw data of UHPLC-TOF/MS analysis was processed by Agilent Mass Hunter Qualitative Analysis B.06.00 (Agilent Technologies, Santa Clara, USA). Electrospray ionization (ESI) mass spectra were acquired in negative mode. The results were recorded with the following ESI source parameters: end plate offset voltage of 1000 V, capillary voltage of 3500 V, nebulizer of 35 psi and dry gas flow of 8.0 L/min at 325℃. Extracted ion chromatogram (EIC) was used as a mode to extract the target iron.

The chromatographic separation was carried out on an ACQUITY UPLC BEH shield RP18 column (100 mm × 2.1 mm I.D., 1.7 μm, Waters Corp., Milford, MA, USA) with a constant temperature of 30 °C. The flow rate was 0.35 mL/min and the injection volume was 3 μL. The mobile phase consisted of 0.1% formic acid in methanol (A) and 0.1% formic acid in acetonitrile (B). A linear gradient was optimized as follows: 0–8 min, 10–20% B; 8–14 min, 20–80% B; 14–14.5 min, 80–10% B; and finally equilibrated with 10% B for 1.5 min.

2.7. FT-IR and 2D IR analysis

The FT-IR spectra were collected and analyzed on a Cary 600 FT-IR spectrometer (Agilent Technologies, Santa Clara, USA) (Sun, Lin, Wu, & Siesler, 2008). KBr powder was preprocessed to dry at 130 °C for 4 h. Each EBN sample was polished and mixed thoroughly with 25 mg KBr and made into pellets. The KBr based pellets were put into a thin disk to be compressed by establishing the pressure at 10 t for about 5 min. Half millimeter tablets were then made out for FT-IR spectra scanning. The tablets and KBr should be exposed to an infrared lamp, to avoid absorbing moisture from the air. Infrared scan was performed at 64 times/min with a wavenumber from 4000 cm^{-1} to 400 cm^{-1}. The baseline correction, normalization and the band areas were obtained using the same software program. The generalized 2D correlation analysis was applied by the 2D shige software developed by Shigeaki Morita (Kwansei-Gakuin University, Japan). For easy display and observation, the correlation maps of 2D IR were shown as grayscale images in the following results. Schematic contour maps of 2D synchronous correlation spectra were formed from the primary spectra of

different samples processed with gradient temperature from 25 to 65 °C. And they reflected the difference between the different samples more directly than the second derivative spectra and wavelet transform spectrum.

2.8. ^1H NMR analysis

The products with different colors were analyzed by ^1H NMR. ^1H NMR experiments were performed on a Bruker Ascend LH 600 MHz NMR spectrometer (Bruker Corporation, Karlsruhe, Germany) operating at NMR frequency of 600 MHz for ^1H NMR. They were equipped with a 5 mm CryoProbe (CP DCH 600S3 C/H-D-05 Z) in deuterated methanol solution at 298 K. All ^1H (600 MHz) spectra results were recorded with chemical shifts in δ (ppm) and coupling constants (*J*) in hertz (Hz).

2.9. SDS-PAGE analysis

Samples of white EBNs, natural blood-red EBNs, blood-red EBNs of unclear origin, artificially fumigated blood-red EBNs after a strong reaction with concentrated HCl, $NaNO_2$ and $NH_3{\cdot}H_2O$ for only 3 h, artificially fumigated blood-red EBNs after a normal reaction with 2% HCl, $NaNO_2$ and $NH_3{\cdot}H_2O$ for 24 h, were used for SDS-PAGE analysis. Proteins in EBNs were extracted using 0.01 M Tris-HCl buffer at pH 6.8. The samples were centrifuged at 12,000 rpm for 10 min, and the precipitate was dissolved in water (200 μL) and then quantified using Cary 600-UV spectrophotometer (Agilent Technologies, Santa Clara, USA). Fifty microliters of protein were separated on a 10% SDS-PAGE gel with a maker (20–250 kDa) for 3 h at 80 V. The gel was stained with Coomassie brilliant blue and bleached overnight with destaining solution containing 10% acetic acid and 30% methanol, and then photographed by Bio-Rad Gel Doc XR+ Imaging System (BioRad, Hercules, CA, USA).

3. Results and discussion

3.1. Artificial color change of L-tyrosine and EBN

The core of chemical mechanism in PCRE is a kind of deformation of amino acids through chemical intervention with $NaNO_2$, HCl and $NH_3{\cdot}H_2O$. Since the conjugated double bonds of the benzene ring generate color reaction easily, tyrosine is the easiest amino acid to react and abundant in EBNs, so it accordingly becomes the important observe target. L-tyrosine acted as an example to propose the hypothesis, because its aromatic ring could be changed and the other chromophores could be added in different chemical environments (Slominski, Zmijewski, & Pawelek, 2012). Therefore, nitrification (product: 3-Nitro-L-tyrosine), primary amine diazotization (product: 2-Hydroxy-3-(4-hydroxy-3-nitrophenyl)-propionic acid), and phenol-keto tautomerism (Kachurovskaya, Zhidomirov, Hensen, & VanSanten, 2003; Stępień, Latos-Grazyński, & Szterenberg, 2007) (products: Keto form of 3-nitro-L-tyrosine and 2-hydroxy-3-(4-hydroxy-3-nitrophenyl)-propionic acid) were the main theoretical reaction products throughout the PCRE. As shown in Fig. 2A, saturated L-tyrosine solutions were fumigated with Wong's method (But et al., 2013; Paydar et al., 2013), and the products presented yellow. When taking further alkaline fumigation with $NH_3{\cdot}H_2O$, the products' colors turned from yellow to red. The colors were deepened with the time extension of fumigation from 24 h to 48 h. This phenomenon

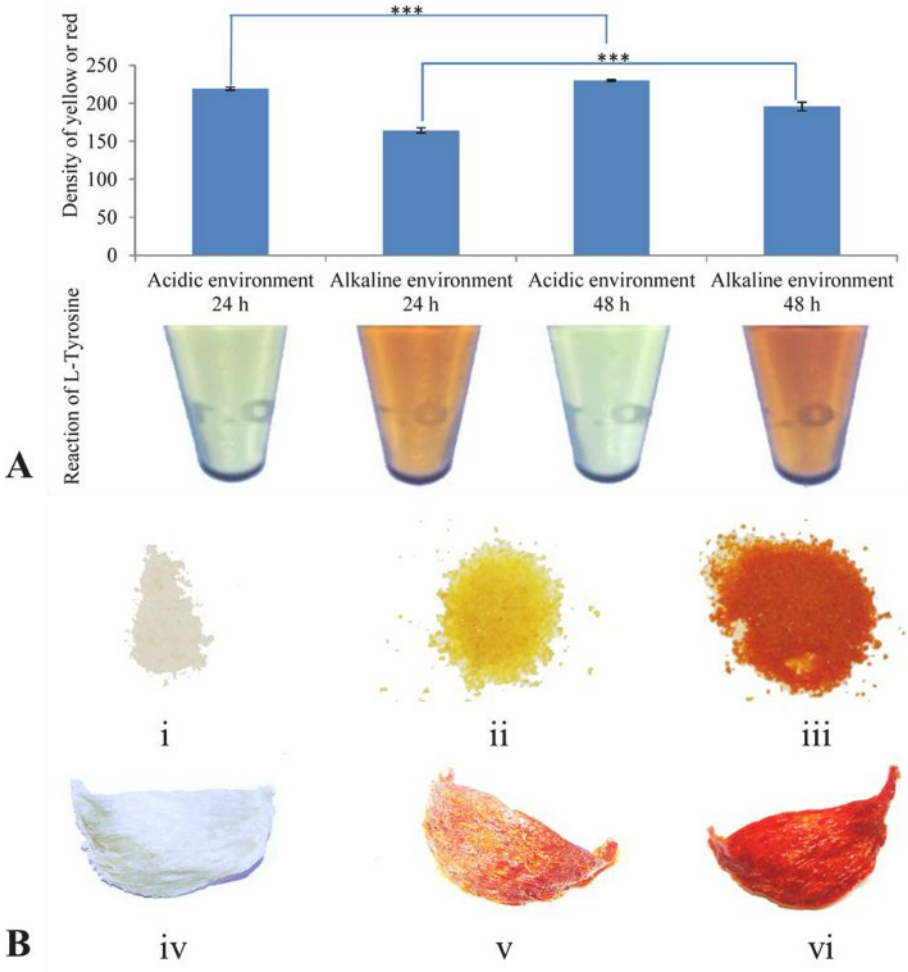

Fig. 2. The color change reactions on L-tyrosine (A) and white EBNs (B) under different conditions. A: Acidic environment is processed by 2% HCl and $NaNO_2$, alkaline environment is processed by 2% HCl, $NaNO_2$ and $NH_3{\cdot}H_2O$ (***: Optical density detection, $n = 6$, $p < 0.01$). B: i turns into ii, and iv turns into v in the process of 2% HCl and $NaNO_2$; i turns into iii, and iv turns into vi, in the process of 2% HCl, $NaNO_2$ and $NH_3{\cdot}H_2O$. $NH_3{\cdot}H_2O$ doesn't mix with the HCl, and the filter paper stained with $NH_3{\cdot}H_2O$ is hanged at the top of the bottle, then a large amount of white smoky gas is generated.

suggested that the reaction proceeded very slowly, even if the reacted conditions were much more intense than the natural formation environment.

The color reaction needed to reproduce on the EBNs, so EBN samples were prepared as two forms, powder and complete one, and fumigated directly by the same method. As shown in Fig. 2B, yellow powder (Fig. 2B-ii) and red complete one (Fig. 2B-v) were generated using Wong's method on the white EBNs, while red powder (Fig. 2B-iii) and deep red complete one (Fig. 2B-vi) were obtained by the alkaline fumigation with additional $NH_3{\cdot}H_2O$ on the white EBNs. It determined that L-tyrosine produced two types of substances showing yellow and red respectively. It should be emphasized that the yellow substance also presented red in the complete nest. This phenomenon enabled us to focus on the chromophores and conjugate changes at the peptide chain, since the folded spatial structure is a property of the protein.

3.2. Detection of the reddening substances with UHPLC-TOF/MS and UV spectrophotometer

Direct use of the UHPLC-TOF/MS was a sensitive and intuitive method to observe the formation and change of target compounds. Two products produced by the reaction of L-tyrosine that caused color change were detected by using UHPLC-TOF/MS. As shown in Fig. 3A, four chemical components were detected on EIC and marked as M1 ~ 4. Preliminary results showed that $C_9H_{10}N_2O_5$ and $C_9H_9NO_6$ predicted in the hypothesis of the EBN reddening mechanism were determined successfully, the amount of M1 ($C_9H_{10}N_2O_5$) increased and the amount of M3 ($C_9H_9NO_6$) decreased obviously from yellow solution to red solution. The compound M2 ($C_9H_9NO_6$), having the same chemical structural formula with M3, existed in both yellow solution and red solution with trace amount, which inferred to be 2-hydroxy-3-(4-hydroxy-2-nitrophenyl)-propionic acid. M4 ($C_9H_8N_2O_8$) was inferred to be 2-hydroxy-3-(4-hydroxy-3,5-dinitrophenyl)-propionic acid and only existed in red solution, and their derived chemical structural formulas were shown in Fig. 3B. Furthermore, yellow and red solutions were analyzed with UV spectrophotometer. As shown in Fig. 3C, the results showed that yellow solution was proved with a benzene ring, because it had an absorption peak at 358 nm, while the red solution didn't have this peak.

3.3. Structure identification of the reddening substances to support the hypothesis of color formation mechanism

The results of UHPLC-TOF/MS and UV spectrophotometer support the hypothesis, through proving the rationality of the synthetic route in Fig. 1B. However, more evidence should be collected to determine the detailed structure of reddening substances. After being separated with paper chromatography, yellow and red solutions were identified by ^1H NMR. Yellow solution showed 3 signals (2-H, 5-H, 6-H) in the range of benzene ring (Politzer, Seminario, & Bolduc, 1989) from 7.5 ppm to 8.5 ppm, while they didn't exist in the spectrum of red one. Instead, the new 3 signals (2-H, 5-H, 6-H) from 6.0 ppm to 7.5 ppm appeared in the spectrum of red one (Fig. S2, see supplementary materials). The yellow solution had a signal of –OH at the benzene ring from 9.5 ppm to 10 ppm, and this signal disappeared in the red solution. So, these results proved that the benzene ring was changed after fumigating with $NH_3{\cdot}H_2O$. The NMR signals showed the clear chemical shifts and splitting parameters, which closely matched the theoretical spectra calculated using the Advanced Chemistry Development (ACD/Labs) software V11.01 (c 1994–2011 ACD/Labs Inc) (Kouamé et al., 2013). In this study, we compared the NMR signals with that of the reported chemicals under similar chemical environment (3,5-Cyclohexadiene-1,2-dione,4-(1,1-dimethylethyl)-,2-oxime; 3,5-Cyclohexadiene-1,2-dione,4-methyl-,2-oxime; 3,5-Cyclohexadiene-1,2-dione,4-(1,1-dimethylethyl)-,2-(O-methyloxime),(E)-(9CI)), the results showed that the NMR signals serve to characterize the crystal chemistries, and proved the existence of a basic ring named 2, 4-cyclohexadien-1-one-6-*aci*-nitro- in the products

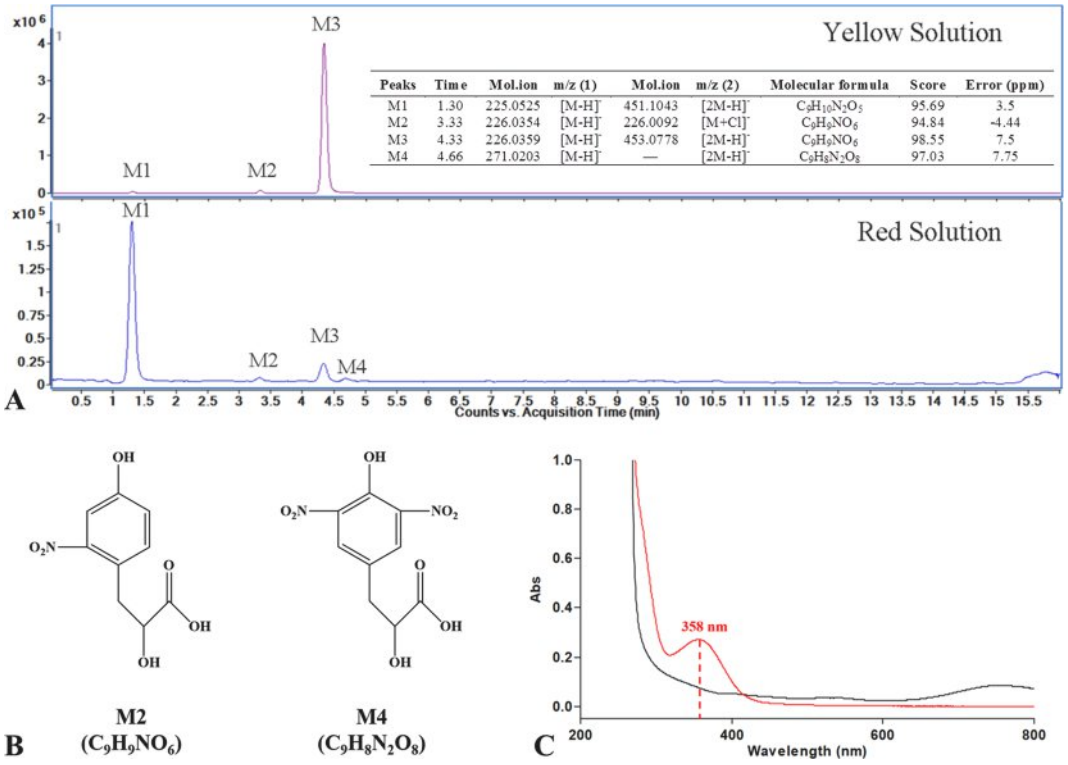

Peaks	Time	Mol.ion	m/z (1)	Mol.ion	m/z (2)	Molecular formula	Score	Error (ppm)
M1	1.30	225.0525	$[M-H]^-$	451.1043	$[2M-H]^-$	$C_9H_{10}N_2O_5$	95.69	3.5
M2	3.33	226.0354	$[M-H]^-$	226.0092	$[M+Cl]^-$	$C_9H_9NO_6$	94.84	-4.44
M3	4.33	226.0359	$[M-H]^-$	453.0778	$[2M-H]^-$	$C_9H_9NO_6$	98.55	7.5
M4	4.66	271.0203	$[M-H]^-$	—	$[2M-H]^-$	$C_9H_8N_2O_8$	97.03	7.75

Fig. 3. UHPLC-TOF/MS (A) and UV absorption analysis (C) of L-tyrosine reacted products, with the derived chemical structural formulas of M2 ($C_9H_9NO_6$) and M4 ($C_9H_8N_2O_8$) (B). C: The red line and the black line represent the UV absorption of yellow solution and red solution respectively. The red line has an absorption peak at 368 nm, which proves to have a benzene ring. (For interpretation of the references to color in this figure legend, the reader is referred to the web version of this article.)

of red solution. Moreover, the interesting phenomenon was that there was a very similar composition exiting in the red solution with a low content. The chemical shifts (frequency) of the 3 signals reduced 0.5 ppm. This was a new important evidence to support the mechanism hypothesis that there are two reddening substances called keto form of 3-nitro-L-tyrosine and 2-hydroxy-3-(4-hydroxy-3-nitrophenyl)-propionic acid, as shown in Fig. 1B. Based on the UHPLC-TOF/MS and UV absorption analysis results, the inferred reaction process led the L-tyrosine to yellow and red solutions were shown in Fig. 4A.

3.4. Reddening substances detection in enzymatic hydrolyzed EBNs and fake blood-red EBNs using CPA

The detection of the reddening substances and the mechanism of the color formation on EBNs have been performed and showed above. However, the reddening substances were also required to be verified in the natural and fake blood-red EBNs. So color substances from the hydrolyzed solution of the EBNs was analyzed by UHPLC-TOF/MS using the same experimental conditions.

In our hypothesis, we believed that almost all tyrosine in the peptide chain can participate in the color reaction. Therefore, how to specifically obtain a large amount of hydrolyzed 3-nitro-L-tyrosine or other colored compounds was very important, otherwise our chemical equipment may not be able to detect it. In our study, to ensure that the target compounds might be detected by UPLC-TOF-MS, CPA was used to specifically hydrolyze the carboxyl-containing terminal amino acids on the peptide chain. This is a key technical step that the hypothesis can be verified in this research.

After the enzymatic hydrolysis by CPA (Wu, Zhang, Cao, Xu, & Guo, 2011), natural blood-red EBNs, white EBNs, the artificially fumigated red EBNs and artificially fumigated hydrolysate of white EBNs were all detected. As shown in Fig. 4B, M3 ($C_9H_9NO_6$) existed in natural blood-red EBNs, artificially fumigated red EBNs and artificially fumigated hydrolysate of white EBNs, while M3 hadn't been detected in the white EBNs. Further research showed that M1 ($C_9H_{10}N_2O_5$) was detected in artificially fumigated red EBNs and was not detected in the artificially fumigated hydrolyzed solution of white EBNs, because the ammonia was used to fumigate above the solution and didn't add into the solution, so the ammonia couldn't mix with the solution completely. These results supported the hypothesis that the PCRE can't react completely on the artificial fumigation of EBNs. It was also worth noting that the results confirmed that the aliphatic chains of the important color reaction

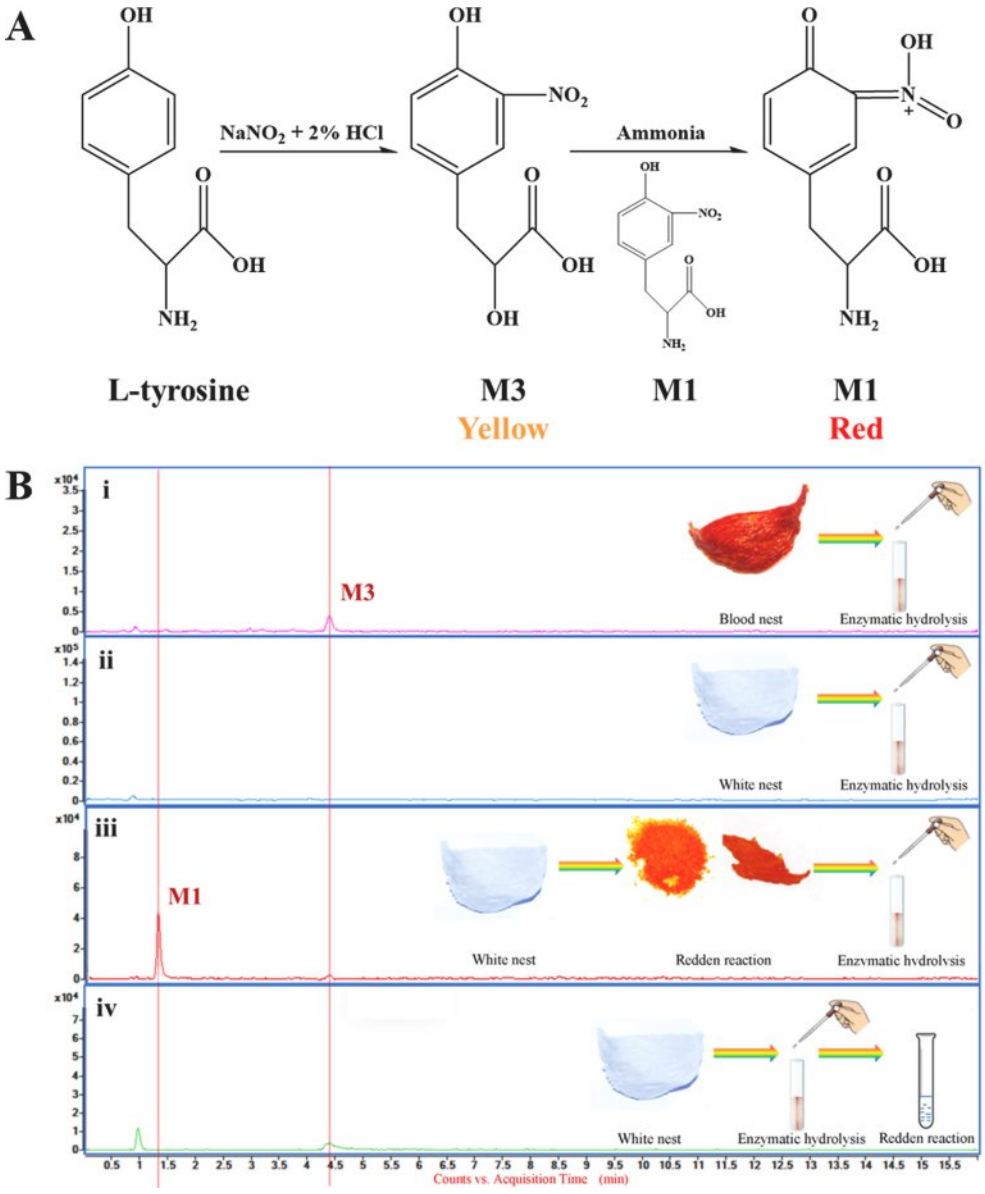

Fig. 4. The reaction process leads the protein L-tyrosine to produce yellow and red solutions (A) and UHPLC-TOF/MS analysis of different EBNs hydrolyzed solutions (B). B: The hydrolyzed solutions are from natural blood-red EBN (i), white EBN (ii), artificially fumigated red EBN (iii) and artificially fumigated hydrolysate of white EBNs (iv). M3 exists in i, iii and iv, and M1 only exists in iii. (For interpretation of the references to color in this figure legend, the reader is referred to the web version of this article.)

products M1 ~ 4 had undergone a diazotization reaction and were finally substituted by hydroxyl or amino groups. Therefore, our hypothesis directly and accurately provided the possible chemical products in the color reaction, so that we could successfully discover the story happened on the protein peptide chain. We further applied the identified chemical markers M1 and M3 to test the blood-red EBN samples from the market (Fig. S3, see supplementary materials). In two of them, M1 and M3 were both detected, which were consistent with the result of artificial red EBN, so these two samples were identified as most likely to be the artificial ones. In the other one of them, only M3 was detected and M1 was not detected, which was consistent with the result of natural EBN, this was identified as most possible to be the natural sample. So, the chemical markers M1 and M3 can provide strong evidence for identification of natural and artificial blood-red EBNs.

3.5. Changing of proteins level between natural and artificial blood-red EBNs

In order to study the changes in protein and special peptide chain reactions during artificially chemical fumigation, SDS-PAGE electrophoresis (Guo, Wu, Liu, Ge, & Chen, 2018; Guo et al., 2017; Marcone, 2005) was performed to detect the protein breakdown. As shown in Fig. 5, the electrophoresis gel result demonstrated that the blood-red EBNs (lane 2–5) had obvious differences with white EBN (lane 1), and the artificially fumigated blood-red EBNs were different from the natural blood-red EBNs with possessing unique protein bands. Between 75 and 100 kDa, there existed 2 bands in artificially fumigated blood-red EBNs (lane 4 and 5), while only 1 band existed in natural blood-red EBNs (lane 2 and 3), which indicated that the emergence of new band may be generated by ruptured peptide chain after treatment of artificial fumigation. This phenomenon has been reported before (Marcone, 2005) that it was very similar in molecular weight compared with the highly allergenic glycosylated ovotransferrin (Williams, Elleman, Kingston, Wilkins, & Kuhn, 1982), protein in eggs which still cannot be confirmed since more evidences are needed.

In order to verify the fracture on the peptide chain, FT-IR was used to detect the white EBNs, natural and artificially fumigated blood-red EBNs. If the protein peptide chain was fractured, the associated signal of chemical groups would be strengthened, such as the group of –COOH. The results were showed in Fig. 6A. And there were four different peaks marked with P1 ~ 4 shown in Fig. 6C, which represented artificially fumigated blood-red EBNs, white EBNs and natural blood-red EBNs. The results provided that many –COOH groups were generated from the fractured protein peptide chain through artificial reaction. And P3 only existed in the artificially fumigated blood-red EBN, representing the stretching vibration of –C═O in hexatomic ring, which also proved that M1 changed to the keto form to show red color. Furthermore, schematic contour maps of 2D correlation spectra of natural and artificially fumigated blood-red EBNs were drawn by the 2D Shige software composed by Shigeaki Morita (Yamasaki & Morita, 2014), which was shown in Fig. 6B. There were two stretching (in ring) peaks appeared in white EBNs at 1600 cm^{-1} and 1455 cm^{-1}, while the stretching (in ring) peaks appeared in natural and artificially fumigated blood-red EBNs were shown at 1580 cm^{-1} and 1454 cm^{-1}. This illustrated that the formation of a carbonyl group was conjugated with the benzene ring in natural and the artificially fumigated blood-red EBNs. What's more, the strong relevant cross peaks only appeared in the artificially fumigated blood-red EBNs (Fig. 6B-iii). This signal showed the conjugation of carbonyl and phenyl was changed in the same direction with increasing temperature. This might be due to incomplete reaction of PCRE on artificially fumigated blood-red EBNs, and oxidation reaction continued under the increasing temperature. In this process, phenol-keto tautomerism led to the cross peaks appeared in the testing of 2D IR. The complicated asynchronous correlation spectra showed that artificially fumigated blood-red EBN has a more complex chemical environment.

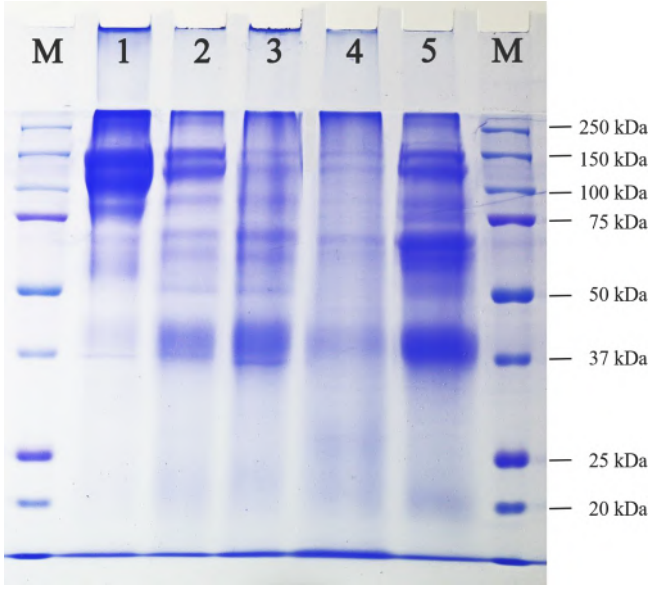

Fig. 5. SDS-PAGE gel electrophoresis analysis of different exacted proteins. Lane 1, white EBN, lane 2, natural blood-red EBN, lane 3, blood-red EBN of unclear origin, lane 4, artificially fumigated blood-red EBN after a strong reaction with concentrated HCl, $NaNO_2$ and $NH_3{\cdot}H_2O$ for only 3 h, lane 5, artificially fumigated blood-red EBN after a normal reaction with 2% HCl, $NaNO_2$ and $NH_3{\cdot}H_2O$ for 24 h. (For interpretation of the references to color in this figure legend, the reader is referred to the web version of this article.)

3.6. Proposal and verification of the reddening reaction of EBNs

To clarify the mechanism of the color formation of blood-red EBNs, a hypothesis mainly based on the process of artificial fumigation was promoted after a large work by reviewing the references, related news and video information. Initially, it should be distinguished that the reddening substance wasn't caused by adding chemical colorants, such as Sudan red, anthocyanins and so on (Pericles, 1982; Tsai, Kuo, & Shih, 2015). In addition, because of the similarity in colorants structure, azo compounds could also dye the EBNs and might be generated during artificial fumigation (Satam, Raut, & Sekar, 2013; Wang et al., 2012). However, it's very disappointing that the organic reagent couldn't easily dissolve reddening substance in subsequent experiments. The reddening substances found in the alkaline hydrolysis process were consistent with our hypothesis. This indicated that the color formation might occur on the peptide chain, and the formation didn't destroy the protein integrity. Moreover, the reddening substances should be in the form of macromolecules. Inspired by a conventional protein color reaction, xanthoproteic reaction (Folin & Denis, 1913), the amino acid contained benzene ring became our research target. Furthermore, we redesigned the color formation mechanism in the framework under experimental conditions. Subsequently, a constructive hypothesis was proposed, involved with a theoretical derivation of various reactions. Some reports also agreed with our hypothesis that the color change is related to the xanthoproteic reaction on L-tyrosine, and verified it by ELISA, which provided a sensitive and fast way using a biological method (Shim & Lee, 2018). In our study, we actually paid more attention to chemical markers that can be accurately determined by modern analytical techniques. The diazotization reaction involving aromatic amine and nitrous acid is the most common color reaction, which should be considered first for the color change. It's also necessary to consider the nitration reaction of aromatic amino acids, especially tyrosine at room temperature. Our research also deduced for the first time the main chemical products that may be produced by the above two important color reactions under different pH conditions. In brief, our study used modern and comprehensive chemical methods to give visual evidence of the reddening

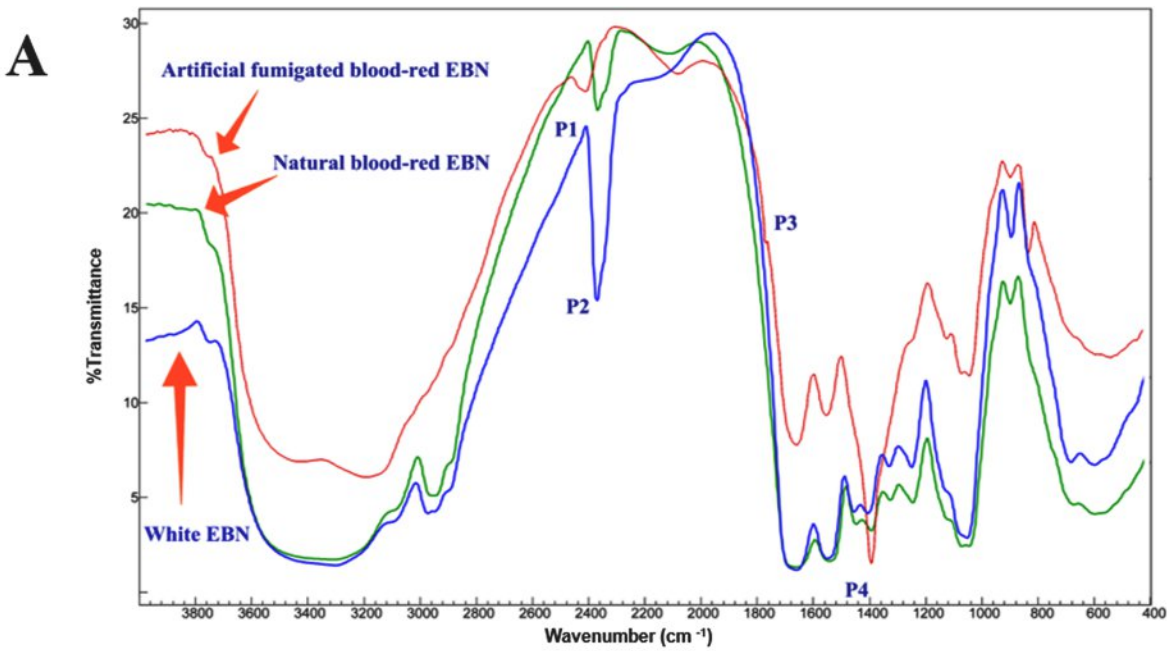

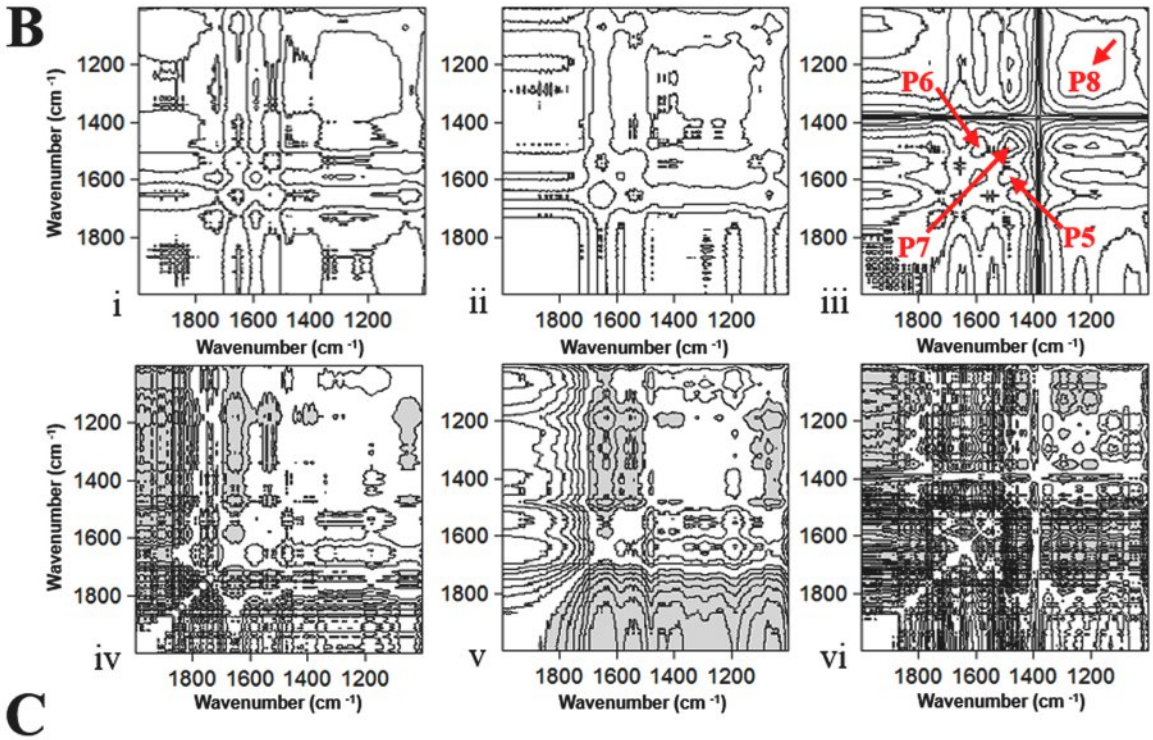

C

No.	Form	Range	Frequency	Groups	Mode of vibration	Intensity
P1	1D	2430~2428 cm^{-1}	2429.5 cm^{-1}	-COOH (-OH)	Doubling and combination	weak
P2	1D	2397~2395 cm^{-1}	2395.8 cm^{-1}	-COOH (-OH)	Doubling and combination	weak
P3	1D	1760~1680 cm^{-1}	1760.0 cm^{-1}	hexatomic ring (-C=O)	stretching	weak
P4	1D	1391~1389 cm^{-1}	1390.0 cm^{-1}	-COOH (-OH)	symmetric stretching	broad
P5	2D	1615~1580 cm^{-1}	1600.0 cm^{-1}	Benzene (C-C in ring)	Auto peaks	medium
P6	2D	1610~1560 cm^{-1}	1580.0 cm^{-1}	Benzene (C-C in ring)	Auto peaks	medium
P7	2D	1460~1450 cm^{-1}	1454.0 cm^{-1}	Benzene (C-C in ring)	Cross peaks	medium/strong
P8	2D	1190~1160	1180.0 cm^{-1}	Aliphatic amines C-NH_2(-C-N)	Cross peaks	medium

Fig. 6. FT-IR (A) and 2D IR (B) analysis of three kinds of EBNs and the detailed information of peaks marked in the IR analysis (C). B: i and iv represent white EBN, ii and v represent natural blood-red EBN, and iii and vi represent artificially fumigated blood-red EBN. i, ii and iii define the positive correlation intensities in the 2D correlation maps, iv, v and vi define the negative correlation intensities in the 2D correlation maps. The red arrows pointing strong relevant cross peaks only appear in the artificially fumigated blood-red EBN. (For interpretation of the references to color in this figure legend, the reader is referred to the web version of this article.)

substance, and further revealed the difference between natural and artificially fumigated blood-red EBNs.

To validate our hypothesis about the color formation mechanism of blood-red EBNs, we simulated an artificial fake way using a single compound L-tyrosine as a reaction substrate. The reaction results were detected by UHPLC-TOF/MS, and the reddening substances were confirmed by ^{1}H NMR, FT-IR, *etc*. This approach could effectively avoid two experimental difficulties: on the one hand, it was unable to find the target reaction products because of the complex substrates and reaction process. On the other hand, it was unable to identify the target reaction products with modern analytical instruments since the insufficient unknown substrates resulting in low product concentrations. In addition, the substitution of L-tyrosine saved a lot of sample resources and greatly reduced costs. In view of a large number of adulterants in the market, it was an effective way to avoid analysis troubles caused by the fake samples. It gave a clear purpose on the target compounds to be detected in the following research. Thus, the entire verification could be successfully completed in this study.

3.7. Mutual argumentation with multiple methods

A variety of methods were used to verify the color formation hypothesis, including UHPLC-TOF/MS, ^{1}H NMR, FT-IR, 2D IR, SDS-PAGE and UV spectrophotometer. The results of those experiments supported each other and provided an objective answer to the color formation hypothesis in this paper. Benefiting from the characterized information above, the artificial fumigation was detected by UHPLC-TOF/MS, because both M1 ($C_9H_{10}N_2O_5$) and M3 ($C_9H_9NO_6$) appeared in the artificially fumigated blood-red EBNs, and the natural one only contained M3 ($C_9H_9NO_6$). It could also be detected by SDS-PAGE since a distinct protein band appeared at 77 kDa. A relatively simple method was to use FT-IR for wide application, because the peak characterization showed a large number of –COOH groups generate from the fractured protein peptide chain through artificial reaction, and specific peak representing -C═O in hexatomic ring appeared in artificially fumigated blood-red EBN. The more effective approach than other methods should be 2D IR. The artificially fumigated blood-red EBNs had a clear peak in the synchronous correlation spectra, indicating that the conjugation of carbonyl and phenyl changed in the same direction as the temperature increased. The mutual demonstration of multiple methods strongly supported this hypothesis, so that we could propose several detailed quality control approaches for blood-red EBNs in different test scenes. Among them, the use of high-resolution mass spectrometry is the highest priority detection method, because it can detect trace amounts of the quality marker compounds M1 ($C_9H_{10}N_2O_5$) and M3 ($C_9H_9NO_6$). After collecting more samples from different Asian countries, we are also intending to develop a simple technical standard for extensive market detection, such as the use of FT-IR, 2D IR as well as the SDS-PAGE method.

3.8. Developing multiple methods for forgery identification and safety control

The artificially fumigated blood-red EBNs had many different characteristics with natural ones, because of the different products of the fast and incomplete chemical reaction. Therefore, our analytical techniques could be applied to quantify the different products, M1 and M3, as chemical markers to determine whether the EBNs were natural or artificially fake. The nitro groups of M1 and M3 might be removed to form nitrites *in vivo* under the action of enzymatic reductase, such as the quinone reductases in liver, thus exerting unpredictable toxic effects to human body (Beckman, 1996). Additionally, M1 has also been proved to have a toxic effect on the morphology and growth rate of neuroblastoma cells (Chisu et al., 2006). Therefore, the safety control mechanism of blood-red EBNs is urgently needed.

Our method first proposes a new detection strategy to provide consumers with technical certification of natural red EBNs. This study focused on the discovery of the color change mechanism. Our following work will collect samples from Southeast Asia on a large scale, then establish a standardized quality control system and develop a faster and simpler identification method. This still requires more conditions, like the standard process for hydrolysis of CPA, detection limit of chemical markers, *etc.*, now we are actively promoting it.

4. Conclusion

The blood-red EBNs are currently misunderstood to be all chemically treated and strictly prohibited exporting to market. Completely denying blood-red EBNs is unobjective and unfair, so a scientific method to identify and evaluate blood-red EBNs is necessary. Our study discovers the reddening mechanism of natural and artificially fumigated EBNs, and establishes a comprehensive and systematic method of chemical identification for both natural and artificial blood-red EBNs. Therefore, it provides a powerful reference for market and customers to authenticate and determine the value of blood-red EBNs effectively.

CRediT authorship contribution statement

Chun-Song Cheng: Conceptualization, Methodology, Investigation, Formal analysis, Writing - original draft, Visualization. **Chi-Chou Lao:** Investigation, Formal analysis, Resources. **Qi-Qing Cheng:** Formal analysis, Data curation, Writing - original draft, Writing - review & editing, Visualization. **Zi-Ling Zhang:** Investigation. **Jing-Guang Lu:** Investigation. **Jian-Xin Liu:** Investigation. **Hua Zhou:** Conceptualization, Methodology, Supervision, Writing - review & editing, Project administration.

Declaration of Competing Interest

The authors declare that they have no known competing financial interests or personal relationships that could have appeared to influence the work reported in this paper.

Acknowledgements

This research was funded by the Science and Technology Development Fund, Macao SAR (File no. 0061/2019/AGJ, 0027/2017/AMJ, 062/2017/A2, 037/2014/A1).

Appendix A. Supplementary data

Supplementary data to this article can be found online at https://doi.org/10.1016/j.foodchem.2021.129454.

References

Beckman, J. S. (1996). Oxidative damage and tyrosine nitration from peroxynitrite. *Chemical Research in Toxicology, 9*(5), 836–844. https://doi.org/10.1021/tx9501445.

But, P. P. H., Jiang, R. W., & Shaw, P. C. (2013). Edible bird's nests – How do the red ones get red? *Journal of Ethnopharmacology, 145*(1), 378–380. https://doi.org/10.1016/j.jep.2012.10.050.

Ceriotti, G., & Spandrio, L. (1957). Colorimetric determination of tyrosine. *The Biochemical Journal, 66*(4), 607–610. https://doi.org/10.1042/bj0660607.

Chan, G. K. (2018). Searching for Active Ingredients in Edible Bird's Nest. Journal of Complementary Medicine & Alternative Healthcare, 6(2). 10.19080/jcmah.2018.06.555683.

Chisu, V., Manca, P., Lepore, G., Gadau, S., Zedda, M., & Farina, V. (2006). Testosterone induces neuroprotection from oxidative stress. Effects on catalase activity and 3-nitro-L-tyrosine incorporation into α-tubulin in a mouse neuroblastoma cell line. Archives Italiennes de Biologie. 10.4449/aib.v144i2.882.

Christianson, D. W., & Lipscomb, W. N. (1989). Carboxypeptidase A. *Accounts of Chemical Research, 22*(2), 62–69. https://doi.org/10.1021/ar00158a003.

Ferrer, I., & Thurman, E. M. (2007). Multi-residue method for the analysis of 101 pesticides and their degradates in food and water samples by liquid chromatography/time-of-flight mass spectrometry. *Journal of Chromatography A, 1175*(1), 24–37. https://doi.org/10.1016/j.chroma.2007.09.092.

Folin, O., & Denis, W. (1913). a New (colorimetric) method for the determination of uric acid in blood. *Journal of Biological Chemistry, 13*(4), 469–475.

Goh, D. L. M., Chew, F. T., Chua, K. Y., Chay, O. M., & Lee, B. W. (2000). Edible "bird's nest" – Induced anaphylaxis: An under-recognized entity? *Journal of Pediatrics, 137*(2), 277–279. https://doi.org/10.1067/mpd.2000.107108.

Guo, L., Wu, Y., Liu, M., Ge, Y., & Chen, Y. (2018). Rapid authentication of edible bird's nest by FTIR spectroscopy combined with chemometrics. *Journal of the Science of Food and Agriculture*. https://doi.org/10.1002/jsfa.8805.

Guo, L., Wu, Y., Liu, M., Wang, B., Ge, Y., & Chen, Y. (2014). Authentication of edible bird's nests by TaqMan-based real-time PCR. *Food Control, 44*, 220–226. https://doi.org/10.1016/j.foodcont.2014.04.006.

Guo, L., Wu, Y., Liu, M., Wang, B., Ge, Y., & Chen, Y. (2017). Determination of edible bird's nests by FTIR and SDS-PAGE coupled with multivariate analysis. *Food Control, 80*, 259–266. https://doi.org/10.1016/j.foodcont.2017.05.007.

Kachurovskaya, N. A., Zhidomirov, G. M., Hensen, E. J. M., & VanSanten, R. A. (2003). Cluster model DFT study of the intermediates of benzene to phenol oxidation by N2O on FeZSM-5 zeolites. *Catalysis Letters, 86*(1–3), 25–31. https://doi.org/10.1023/A:1022642521434.

Kouamé, P.-K., Jacques, C., Bedi, G., Silvestre, V., Loquet, D., Barillé-Nion, S., … Tea, I. (2013). Phytochemicals isolated from leaves of chromolaena odorata: Impact on viability and clonogenicity of cancer cell lines. *Phytotherapy Research, 27*(6), 835–840. https://doi.org/10.1002/ptr.v27.610.1002/ptr.4787.

Lin, J.-R., Zhou, H., Lai, X.-P., Hou, Y., Xian, X.-M., Chen, J.-N., … Dong, Y. (2009). Genetic identification of edible birds' nest based on mitochondrial DNA sequences. *Food Research International, 42*(8), 1053–1061. https://doi.org/10.1016/j.foodres.2009.04.014.

Marcone, M. F. (2005). Characterization of the edible bird's nest the "Caviar of the East". *Food Research International, 38*(10), 1125–1134. https://doi.org/10.1016/j.foodres.2005.02.008.

Paydar, M., Wong, Y. L., Wong, W. F., Hamdi, O. A. A., Kadir, N. A., & Looi, C. Y. (2013). Prevalence of nitrite and nitrate contents and its effect on edible bird nest's color. *Journal of Food Science, 78*(12), T1940–T1947. https://doi.org/10.1111/jfds.2013.78.issue-1210.1111/1750-3841.12313.

Pericles, M. (1982). Anthocyanins As Food Colors. Elsevier. 10.1016/B978-0-12-472550-8.X5001-X.

Politzer, P., Seminario, J. M., & Bolduc, P. R. (1989). A proposed interpretation of the destabilizing effect of hydroxyl groups on nitroaromatic molecules. *Chemical Physics Letters, 158*(5), 463–469. https://doi.org/10.1016/0009-2614(89)87371-3.

Quiocho, F. A., & Lipscomb, W. N. (1971). Carboxypeptidase A: A Protein and an Enzyme (pp. 1–78). 10.1016/S0065-3233(08)60278-8.

Satam, M. A., Raut, R. K., & Sekar, N. (2013). Fluorescent azo disperse dyes from 3-(1,3-benzothiazol-2-yl)naphthalen-2-ol and comparison with 2-naphthol analogs. *Dyes and Pigments, 96*(1), 92–103. https://doi.org/10.1016/j.dyepig.2012.07.019.

Shim, E.-K.-S., & Lee, S.-Y. (2018). Nitration of tyrosine in the mucin glycoprotein of edible bird's nest changes its color from white to red. *Journal of Agricultural and Food Chemistry, 66*(22), 5654–5662. https://doi.org/10.1021/acs.jafc.8b01619.

Shim, E. K. S., Chandra, G. F., Pedireddy, S., & Lee, S. Y. (2016). Characterization of swiftlet edible bird nest, a mucin glycoprotein, and its adulterants by Raman microspectroscopy. *Journal of Food Science and Technology, 53*(9), 3602–3608. https://doi.org/10.1007/s13197-016-2344-3.

Slominski, A., Zmijewski, M. A., & Pawelek, J. (2012). L-tyrosine and L-dihydroxyphenylalanine as hormone-like regulators of melanocyte functions. *Pigment Cell & Melanoma Research, 25*(1), 14–27. https://doi.org/10.1111/j.1755-148X.2011.00898.x.

Stępień, M., Latos-Grazyński, L., & Szterenberg, L. (2007). 22-Hydroxybenziporphyrin: Switching of antiaromaticity by phenol-keto tautomerization. *Journal of Organic Chemistry, 72*(7), 2259–2270. https://doi.org/10.1021/jo0623437.

Sun, B., Lin, Y., Wu, P., & Siesler, H. W. (2008). A FTIR and 2D-IR spectroscopic study on the microdynamics phase separation mechanism of the poly(N-isopropylacrylamide) aqueous solution. *Macromolecules, 41*(4), 1512–1520. https://doi.org/10.1021/ma702062h.

Tsai, C. F., Kuo, C. H., & Shih, D. Y. C. (2015). Determination of 20 synthetic dyes in chili powders and syrup-preserved fruits by liquid chromatography/tandem mass spectrometry. *Journal of Food and Drug Analysis, 23*(3), 453–462. https://doi.org/10.1016/j.jfda.2014.09.003.

Wang, J. Q., Liu, Y. H., Chen, M. W., Dmitri, V. L. L., Inoue, A., & Perepezko, J. H. (2012). Excellent capability in degrading azo dyes by MgZn-based metallic glass powders. *Scientific Reports, 2*, 1–6. https://doi.org/10.1038/srep00418.

Williams, J., Elleman, T. C., Kingston, I. B., Wilkins, A. G., & Kuhn, K. A. (1982). The primary structure of hen ovotransferrin. *European Journal of Biochemistry, 122*(2), 297–303. https://doi.org/10.1111/ejb.1982.122.issue-210.1111/j.1432-1033.1982.tb05880.x.

Wong, Z. C. F., Chan, G. K. L., Dong, T. T. X., &Tsim, K. W. K. (2018). Origin of Red Color in Edible Bird's Nests Directed by the Binding of Fe Ions to Acidic Mammalian Chitinase-like Protein. Journal of Agricultural and Food Chemistry, 66(22), 5644–5653. research-article. 10.1021/acs.jafc.8b01500.

Wu, S., Zhang, C., Cao, R., Xu, D., & Guo, H. (2011). pH-dependent reactivity for glycyl-L-tyrosine in carboxypeptidase A catalyzed hydrolysis. *The Journal of Physical Chemistry B, 115*(34), 10360–10367. https://doi.org/10.1021/jp2046504.

Xian, X. M., Hou, Y., Lin, J. R., Huang, S., Lai, X. P., & Chen, J. N. (2010). Study on degradation of protein of the edible birds' nest (Aerodramus) in vitro. Retrieved from *Journal of Chinese Medicinal Materials, 33*(11), 1760–1763 http://www.ncbi.nlm.nih.gov/pubmed/21434440.

Yamasaki, H., & Morita, S. (2014). Identification of the epoxy curing mechanism under isothermal conditions by thermal analysis and infrared spectroscopy. *Journal of Molecular Structure, 1069*, 164–170. https://doi.org/10.1016/j.molstruc.2014.01.037.

Yang, M., Cheung, S. H., Li, S. C., & Cheung, H. Y. (2014). Establishment of a holistic and scientific protocol for the authentication and quality assurance of edible bird's nest. *Food Chemistry, 151*, 271–278. https://doi.org/10.1016/j.foodchem.2013.11.007.